Binding of Ca^{2+} to Sulfogalactosylceramide and the Sequential Effects on the Lipid Dynamics†

Susanne Tupper,‡ Patrick T. T. Wong,§ and Nongnuj Tanphaichitr*,‡

Human IVF Labs, Reproductive Biology Unit, Loeb Research Institute, Ottawa Civic Hospital, and Departments of Obstetrics and Gynecology and of Biochemistry, University of Ottawa, and Steacie Institute of Molecular Sciences, National Research Council of Canada, Ottawa, Ontario, Canada

Received April 22, 1992; Revised Manuscript Received August 19, 1992

ABSTRACT: Sulfogalactosylceramide (SGC) is a sulfoglycolipid commonly found in epithelial cells and most animal germ cells. Its cellular function in sperm is unknown, although it has been implicated in cation transport in epithelial cells. The purpose of this study was to determine the lipid dynamic effects of Ca^{2+} binding to SGC. High-pressure Fourier transform infrared spectroscopy was used in this study. Our spectral results showed that Ca^{2+} bound to the sulfate moiety of SGC. Moreover, Ca^{2+} binding weakened the hydrogen bonding of the polar head region of SGC and the hydrocarbon chains became more disordered as revealed by an increase in the correlation field splitting pressure of SGC. Consequently, Ca^{2+} binding to SGC would increase the fluidity of SGC multibilayers. However, the presence of an α-hydroxyl group on the SGC fatty acid was found to strengthen the hydrogen bonding of the polar head region and as a consequence reduced the Ca^{2+}-enhanced hydrocarbon chain disorder. Experimental approaches, described in this paper, serve as a model for further studies of the effects of Ca^{2+} binding on the dynamics of membranes containing SGC or other sulfatides.

Sulfogalactosylceramide (SGC),[1] often referred to as cerebroside sulfate (Figure 1), is a glycosphingolipid that is abundant in several animal tissues including brain (Norton & Autilo, 1966), retina (Dreyfus et al., 1978), kidney (Martensson, 1963; Bentley et al., 1976), skeletal muscle (Sung et al., 1973), and testis of birds, fish, reptiles, amphibians, and certain mammals including humans (Murray & Narasimhan, 1990; Ishizuka & Yamakawa, 1974). In brain, SGC may function in myelin formation (Morrel et al., 1972). SGC is present in the outer leaflet of the plasma membrane bilayer (Hakomori, 1981) and may play a role in the maintenance of the electrolyte balance of biological membranes (Hakomori, 1981; Karlsson et al., 1971, 1974). Since SGC possesses a negative charge, it may readily bind to cations or amines, resulting in electrical neutrality of the molecule (Farooqui, 1978). Among several cations tested using the surface radioactivity technique, Ca^{2+} was found to bind with high affinity to SGC while Na^+ and K^+ bind less tightly (Abramson et al., 1967; Quinn & Sherman, 1971). SGC is structurally related to galactosylceramide (GC). As GC has been demonstrated to be involved in the opening of Ca^{2+} channels in oligodendroglia (Dyer & Benjamins, 1990), SGC may also participate in a similar event in other cells.

The dynamics of a lipid can be influenced by the degree of hydrogen bonding by its polar head group. Infrared spectroscopy and X-ray studies of crystalline GC indicate that

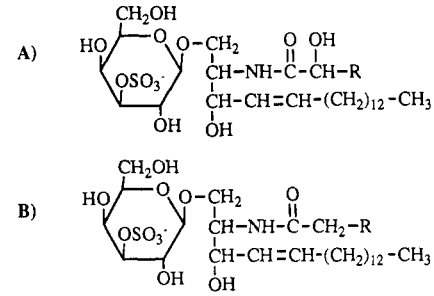

FIGURE 1: Schematic representation of (A) SGC with α-hydroxy fatty acid and (B) SGC with non-hydroxy fatty acid.

GC participates in lateral hydrogen bonds between the amide group and neighboring sugar head groups (Pascher, 1976; Pascher & Sundell, 1977). The presence of an α-hydroxyl group in the GC fatty acyl chain further increases the degree of hydrogen bonding both intermolecularly and intramolecularly (Pascher & Sundell, 1977). A molecular species of SGC with an α-hydroxylated fatty acyl chain also exists (Figure 1A). Differential scanning calorimetry has shown that this α-hydroxyl group in SGC and GC increases stability of the gel phase, presumably because of additional hydrogen bonds (Boggs, 1987). Consequently, a higher proportion of α-hydroxylated to nonhydroxylated species of SGC and GC in the membrane would result in an increase in membrane stability concurrent with a decrease in membrane fluidity/permeability. Consistent with this is the observation that sphingolipids of membranes exposed to physical and chemical stress have a higher proportion of α-hydroxylated species (Pascher & Sundell, 1977). Binding of a cation to the SGC sulfate group, however, may alter the degree of inter/intramolecular hydrogen bonding, which could affect lipid/membrane fluidity and function.

In this study, we asked the question of whether Ca^{2+} binding to SGC multilayers would change the lipid dynamics. High-pressure Fourier transform infrared spectroscopy was used in this study since the technique can determine not only whether Ca^{2+} binds to the sulfate group of SGC but also how this

† This research was partially supported by the Medical Research Council of Canada, Grant MA-10366 (to N.T.).

* To whom correspondence should be addressed at the Reproductive Biology Unit, Ottawa Civic Hospital, 1053 Carling Ave., Ottawa, Ontario K1Y 4E9, Canada; FAX (613) 761-9151; tel (613) 761-4081.

‡ Ottawa Civic Hospital and University of Ottawa.

§ National Research Council of Canada.

[1] Abbreviations: SGC, sulfogalactosylceramide; GC, galactosylceramide; SGG, sulfogalactosylacylalkylglycerol; αGC, GC with α-hydroxy fatty acid; nGC, GC with non-hydroxy fatty acid; mGC, mixed GC population: ~60% with α-hydroxy fatty acid and ~40% with non-hydroxy fatty acid; SGC-Na^+, Na^+ salt of SGC; SGC-Ca^{2+}, Ca^{2+} salt of SGC; TLC, thin-layer chromatography.

0006-2960/92/0431-11902$03.00/0

binding affects the dynamics of the other parts of the SGC molecule (Auger et al., 1988, 1990; Wong, 1984, 1987; Wong et al., 1985, 1988). In addition, we investigated the effects of fatty acid α-hydroxylation on lipid dynamics.

MATERIALS AND METHODS

Materials

SGC (containing 1.72% Na^+, 1.07% Ca^{2+}) (~60% with α-hydroxy fatty acid and ~40% with non-hydroxy fatty acid); three molecular species of GC (Ca^{2+} content not determined by manufacturer): type I (with α-hydroxy fatty acid) (αGC), type II (with non-hydroxy fatty acid) (nGC), and mixed GC (~60% with α-hydroxy fatty acid and ~40% with non-hydroxy fatty acid) (mGC); D_2O (99.9 atom %); tris-(hydroxymethyl)aminomethane hydrochloride (Tris); and $CaCl_2 \cdot 2H_2O$ were purchased from Sigma Chemical Co. (St. Louis, MO). High-purity natural crystalline α-quartz was obtained from Karl Lambrecht Corp. (Chicago, IL).

According to information from Sigma Chemical Co., SGC and all three types of GC were extracted from bovine brain. The purity of SGC, mGC, nGC, and αGC was 99%, 99%, 98%, and 97%, respectively. We confirmed this purity by ascending thin-layer chromatography (TLC) using the solvent system of $CHCl_3$–MeOH–H_2O (65:25:4 v/v) (data not shown). Glycolipids were detected by their sugar staining with α-naphthol, whereas all lipids, which were exposed to H_2SO_4, were detected by charring (Kates, 1986). Under this TLC condition, all of the GC and SGC samples showed positive α-naphthol staining, verifying that they were glycolipids. No extra bands were observed after charring, indicating no significant impurities from other lipids. The nGC sample gave a single band with its relative R_f value of 0.714, whereas the αGC sample chromatographed as doublets with relative R_f values of 0.679 and 0.667. These αGC doublets presumably represented two αGC molecular species with different fatty acyl chains. Two distinctive bands were observed for the mGC sample with relative R_f values of 0.711 and 0.678. A faint band with the lowest relative R_f value (0.664) was also oberved in the mGC sample. Apparently, the fastest moving band of mGC represented nGC, and the slower moving band and the faint slowest moving band were the αGC doublets. The SGC sample chromatographed as doublets with relative R_f values of 0.539 and 0.559. These SGC doublets presumably represented the sulfatide molecular species with and without an α-hydroxyl group in the fatty acyl chain.

Methods

Removal of Endogenous Ca^{2+} from SGC. A 0.42 mM solution of SGC in 1:1 MeOH–$CHCl_3$ was prepared. Aqueous HCl (0.3 M) was added to the sulfatide solution to give a MeOH:$CHCl_3$:HCl ratio of 1.0:1.0:0.9. The biphasic system was mixed and centrifuged briefly, and the $CHCl_3$ phase was removed by pipetting. The upper MeOH–HCl phase was washed twice with $CHCl_3$ to extract any remaining sulfatide, and the extracts were pooled with the original extraction fraction. The pooled extract was then neutralized with 0.01 N NaOH in MeOH, and the SCG-Na^+ salt (SGC-Na^+) precipitated with acetone (0.5 mL) and dried in vacuo (Kates, 1986).

High-Pressure Infrared Spectroscopy Studies. (*a*) *Sample Preparation.* Approximately 1 mg each of SGC-Na^+, αGC, nGC, and mGC was hydrated (50 wt%) in 50 μM Tris-HCl in D_2O, pH 7.05, to form lipid multilayers. To ensure complete dispersion, the lipid multilayers were heated and vortexed 3–4 times. Multilayers of SGC were also generated in the presence of Ca^{2+} (SGC-Ca^{2+}) by including 1.5 M $CaCl_2$ in the Tris-HCl in D_2O, pH 7.05. This yielded a 0.73 molar ratio of SGC to Ca^{2+}.

Solid samples of SGC-Na^+ and SGC-Ca^{2+} were prepared by lyophilizing the aqueous samples for 24 h, followed by equilibration in a N_2 stream for approximately 72 h. Solid samples of αGC, nGC, and mGC were exposed to a N_2 stream for 1 h to remove any water present.

(*b*) *Fourier Transform Infrared Spectroscopy.* For spectroscopic analysis, individual samples (~0.01 mg) were placed, along with powdered α-quartz (used as an internal pressure calibrant), in a well (0.37-mm diameter) of a stainless steel gasket (0.23-mm thickness), that was then mounted on a diamond anvil cell at room temperature (Wong et al., 1985). A Digilab FTS-60 Fourier transform spectrophotometer was used to measure the infrared spectra at 28 °C using a mercury cadmium telluride detector cooled by liquid N_2. The infrared beam was condensed onto the diamond anvil cell by a sodium chloride lens system.

Infrared spectra of hydrated and anhydrous samples of SGC-Na^+ and SGC-Ca^{2+} were measured as a function of pressure up to 17 kbar. For each spectrum, 512 interferograms were coadded at a spectral resolution of 4 cm^{-1}. The 695-cm^{-1} photon band of the α-quartz was used to determine the hydrostatic pressure in the gasket of the diamond anvil (Wong et al., 1985). Fourier derivation techniques were applied in order to separate unresolvable infrared band contours. Spectral features originating from the vibrational modes of the sulfate group, the amide group, and the hydrocarbon chains were examined.

RESULTS AND DISCUSSION

Both the SGC and mGC used in this study were mixtures of α-hydroxy and non-hydroxy fatty acids. In the present work, the SGC sulfate absorption bands were identified by comparison with the spectra of mGC, the nonsulfated parental compound. The spectra of nGC and αGC were also studied to determine the spectroscopic and structural effects of the α-hydroxyl group.

On the basis that Ca^{2+} binds with higher affinity to SGC than Na^+ (Abramson et al., 1967; Quinn & Sherman, 1971), Na^+ in SGC-Na^+ would be replaced by Ca^{2+} in the presence of an excess of Ca^{2+} to form the SGC-Ca^{2+} salt (SGC-Ca^{2+}). The spectra of SGC-Na^+ and SGC-Ca^{2+} were compared to confirm Ca^{2+} binding of SGC and to determine the dynamic effects of this binding.

Calcium Binding. Our results indicated clearly that Ca^{2+} bound to the sulfate group of SGC. Only two sulfate absorption bands proved to be useful: the asymmetric O═S—O^- stretching mode and the C–O stretching mode of the ester-linked sulfate group. The O═S—O^- symmetric stretching mode, which ranges from 1040 to 1080 cm^{-1} (Bellamy, 1975; Kates, 1986), was not used for the analysis since it overlaps with many C–OH stretching bands from the sugar head group. Also, because of interfering quartz bands, the S–O stretching mode, which ranges from 790 to 830 cm^{-1} (Kates, 1986), was not used.

The asymmetric O═S—O^- stretching band was expected to absorb in the frequency range 1200–1265 cm^{-1} (Kates, 1986). Due to interfering D_2O bands, solid samples were used for the Ca^{2+} binding study. Figure 2 presents the infrared spectra of solid SGC-Na^+, SGC-Ca^{2+}, and mGC in the asymmetric O═S—O^- stretching region at ambient pressure. By comparing the spectra of solid mGC and solid SGC-Na^+,

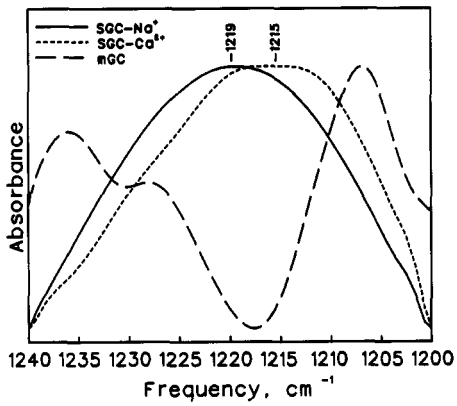

FIGURE 2: Infrared spectra of solid SGC-Na^+, SGC-Ca^{2+}, and mGC in the S=O stretching region (1200–1240 cm^{-1}) at ambient pressure.

the frequency of this stretching mode was observed at ~1220 cm^{-1}. Upon addition of Ca^{2+}, this stretching mode frequency decreased from ~1219 to ~1215 cm^{-1} (Figure 2). This decrease in frequency indicated that Ca^{2+} bound tightly to the sulfate group of SGC. Due to the divalent nature of Ca^{2+}, the cation probably served as a bridge between two SGC head groups.

The stretching region of the C–O group linked to the sulfate group ranges from 930 to 1040 cm^{-1} (Kates, 1986). Comparison of spectral features of hydrated mGC and hydrated SGC-Na^+ in this region revealed an intense band at 990 cm^{-1}, corresponding to the C–O stretching mode. However, no significant change in band frequency or width occurred upon addition of Ca^{2+} to hydrated SGC. Thus, the spectral data indicated that no change in the overall conformation of the sulfate group occurred upon Ca^{2+} binding.

Other regions of the spectrum were analyzed to determine if Ca^{2+} binds to any other groups on SGC. Analysis of the O–H and N–H stretching regions of solid SGC showed no significant changes upon Ca^{2+} addition (data not shown). The results thus showed that Ca^{2+} did not interact with any OH or NH groups. Additionally, Ca^{2+} binding to hydrated mGC did not occur since the GC spectra remained the same in the presence or absence of Ca^{2+} (data not shown).

Amide Group. The amide group of crystalline αGC is highly involved in hydrogen bonding and has a significant effect on the conformational structure of the molecule and the interactions with neighboring molecules (Pascher, 1976; Nyholm et al., 1990). The amide C=O of crystalline αGC is hydrogen bonded with both the hydroxyl group of the sphingosine chain and the 3-OH of the sugar head group from neighboring molecules (Pascher & Sundell, 1977). The hydrogen atom of the amide nitrogen of crystalline αGC forms a bifurcated intramolecular hydrogen bond with the oxygen of the fatty acid α-hydroxyl group and the oxygen of the glycosidic linkage. These interactions restrict the orientation possibilities of any ligands and give rise to the shovel-shape conformation of the αGC molecule (Pascher & Sundell, 1977; Nyholm et al., 1990). In contrast, an absence of the fatty acid α-hydroxyl group would likely cause the interfacial region of the sulfatide structure to be more mobile and would perhaps result in altering its conformation and interactions with neighboring molecules. By comparing the amide I region of solid nGC and αGC spectra, the effect of the α-hydroxyl group on the amide group could be determined.

The amide I C=O stretching region ranges from 1600 to 1670 cm^{-1} (Pimentel & McClellan, 1960). Figure 3 presents the infrared spectra in this region of solid nGC and αGC at ambient pressure. The nGC amide I band occurred at 1646

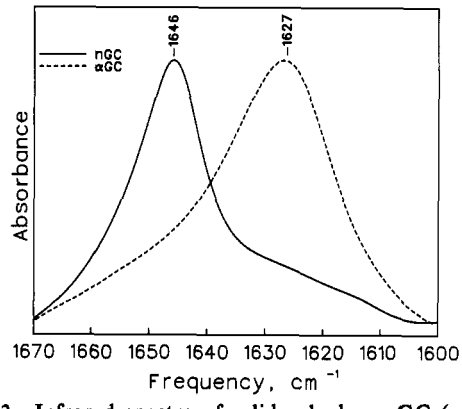

FIGURE 3: Infrared spectra of solid α-hydroxy GC (αGC) and non-hydroxy GC (nGC) in the amide I C=O stretching region (1600–1670 cm^{-1}) at ambient pressure.

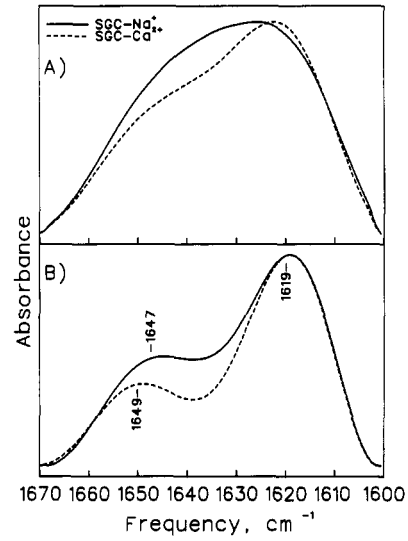

FIGURE 4: (A) Infrared spectra of hydrated SGC-Na^+ and SGC-Ca^{2+} in the amide I C=O stretching region (1600–1670 cm^{-1}). (B) The third-order derivative spectra of SGC-Na^+ and SGC-Ca^{2+} in the amide I C=O stretching region, using a breakpoint of 0.2 in the Fourier domain.

cm^{-1}, indicative of a weakly hydrogen bonded C=O group. In contrast, the αGC amide I band occurred at 1627 cm^{-1}, a frequency associated with a strongly hydrogen-bonded C=O group. The results suggest that the presence of the α-hydroxyl group gave rise to a stronger hydrogen bonding on the amide C=O. This could be due to hydrogen bonding of the α-hydroxyl group with the amide NH, thus causing an increased electron density in the amide C=O and an increase in its dipole moment. Consequently, the amide C=O would strongly hydrogen bond with the sphingosine OH group and 3-OH of the sugar head group, both of neighboring lipid molecules. In contrast, in the absence of the α-hydroxyl group, the amide group would no longer be in a locked conformation and would thus be more mobile. As a consequence, the amide C=O group may be positioned farther away from its hydrogen bonding donors, thus resulting in weaker hydrogen bonding.

The amide I C=O stretching mode of hydrated SGC-Na^+ and SGC-Ca^{2+} at ambient pressure is presented in Figure 4A. Figure 4B presents the third-order derivative spectra of the same region, using a breakpoint of 0.2 in the Fourier domain. The derivatives were obtained to reveal the individual components of the broad bands of Figure 4A. Both the hydrated SGC-Na^+ and SGC-Ca^{2+} spectra were comprised of two components, a low-frequency and a high-frequency band. Since SGC is a mixture of two molecular species

containing α-hydroxy and non-hydroxy fatty acids, two separate amide I absorption modes would be expected. Comparison of the SGC derivative spectra (Figure 4B) with the αGC and nGC spectra (Figure 3) suggests that the high-frequency component, at 1647 cm^{-1}, originated mostly from the non-hydroxy SGC, whereas the low-frequency component, at 1619 cm^{-1}, was from the α-hydroxy SGC.

The presence of a sulfate group affected the amide C=O stretching modes of both SGC molecular species. Sulfation of the 3-OH group of the sugar caused the amide C=O group of the non-hydroxy component of SGC-Na^+ to hydrogen bond somewhat more weakly than in nGC, as reflected by the small increase in vibration frequency from 1646 to 1647 cm^{-1} (Figures 3 and 4B). This small decrease in the strength of hydrogen bonding is most likely the result of an increased intermolecular distance due to charge repulsion contributed by the negatively charged sulfate group. The decrease in frequency of the C=O stretching mode from 1627 to 1619 cm^{-1} of the α-hydroxy component (Figures 3 and 4B) indicates that the presence of the sulfate group caused the amide C=O group of SGC-Na^+ to hydrogen bond even more strongly than in αGC. In contrast to the non-hydroxy component, the negatively charged sulfate group appeared not to cause an increase in intermolecular distance for the α-hydroxy component. Most likely, the stronger intermolecular hydrogen bonding of the amide group in the α-hydroxy component prevented any increase in intermolecular distance and as a result reduced the effect of the sulfate group.

The addition of Ca^{2+} increased the C=O stretching mode frequency of the non-hydroxy SGC from 1647 to 1649 cm^{-1} (Figure 4B). This is most likely due to an increase in the intermolecular distance that results in a further weakening of the intermolecular hydrogen bonding. Moreover, the intensity of the non-hydroxy SGC band decreased upon Ca^{2+} addition (Figure 4), reflecting a reduced transition moment. This decrease in polarity weakened any hydrogen bonding that the amide C=O group was involved in as suggested by the increase in vibrational frequency (Figure 4). The effect of Ca^{2+} addition on the α-hydroxy SGC was negligible, with no change in its C=O stretching frequency. Again, it appears that the stronger intermolecular hydrogen bonding of the amide group in the α-hydroxy component may have prevented any increase in intermolecular distance, and consequently the structure of the amide group was not affected by Ca^{2+} binding to the sulfatide. In contrast, Ca^{2+} binding weakened the hydrogen bonding network of the interfacial region of the SGC molecular species that possesses the non-hydroxy fatty acid.

Methylene Chain Structure. The binding of Ca^{2+} to SGC would be expected to affect not only the amide group but also the hydrocarbon chains. The conformational and orientational order/disorder of the methylene chain structure ultimately determines the fluidity of the multilayer. Information regarding the effects of Ca^{2+} binding and the α-hydroxyl group on the hydrocarbon chains could be useful in predicting the influence of SGC and its α-hydroxy content on membrane fluidity. In the gel phase of lipid bilayers, the methylene chains are largely extended. However, the orientation of these chains is still disordered due to the reorientational fluctuations and twisting and torsion motions. By applying pressure to the lipid multilayers, the mobility of the hydrocarbon chains is slowed down. As the pressure is increased, the intermolecular reorientational fluctuations and twisting and torsion motions are dampened such that the orientations among the hydrocarbon chains become highly ordered (Wong, 1984). When the hydrocarbon chains become nearly perpendicular (i.e., nonequivalent) to each other, a correlation field splitting in the vibrational modes of the methylene chains occurs (Auger et al., 1988, 1990). Therefore, the pressure at which this splitting occurs is an index of the order/disorder of the hydrocarbon chains; greater disorder requires higher pressure to compress the chains into an ordered state.

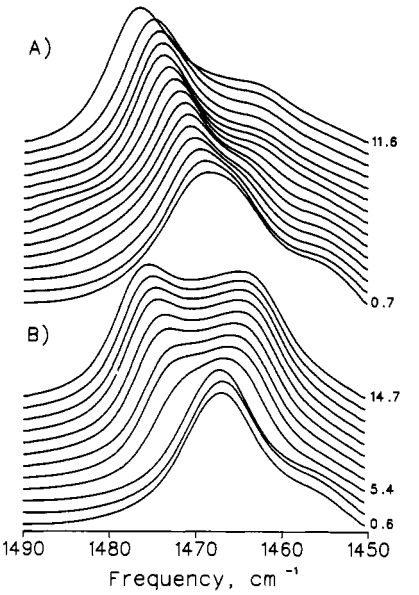

FIGURE 5: Stacked contour plots of the infrared spectra in the CH_2 scissoring region (1450–1490 cm^{-1}) of (A) hydrated non-hydroxy GC (nGC) and (B) hydrated α-hydroxy GC (αGC). The numbers on the right of the plots are pressure values in kbar.

The methylene scissoring bands are located in the region of 1450 to 1490 cm^{-1} and are sensitive to structural differences in hydrocarbon chain packing (Stein & Sutherland, 1953, 1954). Figure 5 presents the stacked contour plots of the infrared spectra of hydrated nGC (A) and αGC (B). At ambient pressure, the intense narrow absorption at 1467 cm^{-1} results from the CH_2 scissoring mode of the fully extended methylene chain. A comparison of the spectra reveals that the baratropic behavior of the methylene scissoring mode was very different in the two types of GC. In the αGC spectra (Figure 5B), a correlation field splitting was induced at pressures above 5.4 kbar. This pressure-induced correlation field splitting of the CH_2 scissoring bands occurs as a result of interchain interactions of the lipid hydrocarbon chains with nonequivalent orientations (Snyder, 1961). These could be intramolecular and/or intermolecular interactions, with the former being predominant at lower pressure (Auger et al., 1988, 1990; Wong, 1987). A single CH_2 scissoring band at ambient pressure (Figure 5B) indicates that the orientation of the methylene chains of αGC was highly disordered due to their significant reorientational fluctuations and twisting and torsion motions. Increasing pressure led to a damping of these reorientational fluctuations and an increase in interchain interactions, which caused the observed correlation field splitting (Figure 5B). In contrast, the correlation field splitting band of the CH_2 scissoring mode is barely noticeable in the nGC spectra (Figure 5A), suggesting that the neighboring methylene chains of the lipid molecules had an approximately equivalent parallel orientation. However, dampening of reorientational fluctuations of the methylene chains at high pressure still occurred in nGC, as indicated by the narrowing of the band with increasing pressure (Figure 5A).

Figure 6 presents the stacked contour plots in the region of the methylene CH_2 scissoring mode of the infrared spectra of SGC-Na^+ (A) and SGC-Ca^{2+} (B). Comparison of the spectra

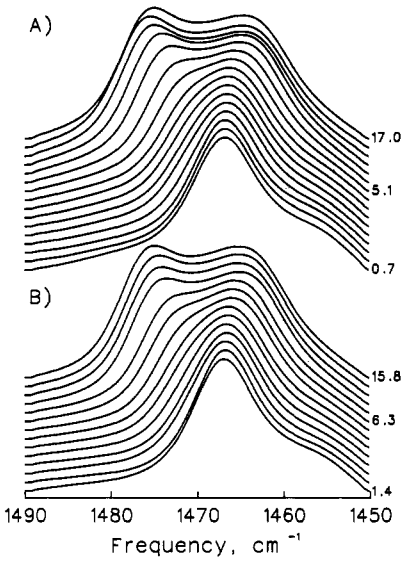

FIGURE 6: Stacked contour plots of the infrared spectra in the CH_2 scissoring region (1450–1490 cm^{-1}) of (A) hydrated SGC-Na^+ and (B) hydrated SGC-Ca^{2+}. The numbers on the right of the plots are pressure values in kbar.

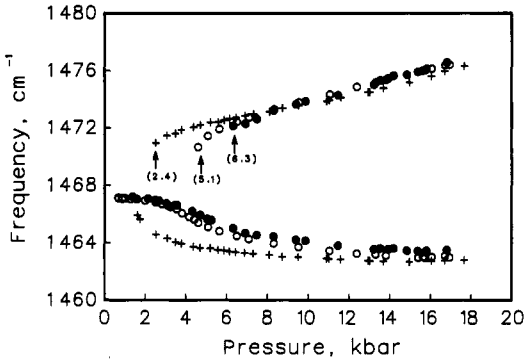

FIGURE 7: Pressure dependence of the frequencies of the CH_2 scissoring region (1460–1480 cm^{-1}) for (○) hydrated SGC-Na^+, (●) hydrated SGC-Ca^{2+}, and (+) hydrated mixed GC (mGC).

reveals that with the exception of the splitting pressure, the baratropic behavior of this band was very similar in the two lipids. As illustrated by a plot of the pressure dependence of the CH_2 scissoring mode frequencies, the correlation field splitting of SGC-Ca^{2+} occurred at 6.3 kbar, a value higher than that of SGC-Na^+ (5.1 kbar) (Figure 7). In contrast, the correlation field splitting of mGC occurred at only 2.4 kbar (Figure 7).

The lower splitting pressure of hydrated mGC suggests that it had highly conformational and orientational ordered chains and would constitute a relatively stable multilayer. The 5.1-kbar splitting pressure of hydrated SGC-Na^+ indicates that the hydrocarbon chains of SGC were significantly more disordered than those in hydrated mGC. The increased disorder may arise from the decreased intermolecular hydrogen bonding of the amide group on the non-hydroxy SGC (Figures 3 and 4B). Moreover, the presence of the negatively charged sulfate group increased the intermolecular distance of the non-hydroxy fatty acyl component (Figures 3 and 4B). Consequently, the space between the methylene chains of neighboring lipid molecules would be larger, and higher pressure would be required to provide the same compression on the methylene chains than that needed for mGC. In contrast, the methylene chains of the α-hydroxy fatty acyl component were probably not affected by the negatively charged sulfate group, given its negligible effect on the amide group of the interfacial region (Figure 4). Therefore, the difference in chain disorder between SGC-Na^+ and mGC was most likely due to the effect of the negatively charged sulfate group on the non-hydroxy SGC-Na^+ component. This conclusion agrees with previous observations from calorimetric studies (Koshy & Boggs, 1983; Boggs et al., 1984) which revealed that SGC with an α-hydroxy fatty acid has a higher order–disorder transition temperature, thus indicating that it has a more ordered gel state than SGC with a non-hydroxy fatty acid.

The 6.3-kbar splitting pressure of SGC-Ca^{2+} indicates that the hydrocarbon chains of SGC-Ca^{2+} were more disordered than those in SGC-Na^+. This agrees with the observation that a divalent cation such as Ca^{2+} causes a decrease in the order–disorder transition temperature of various sulfatides, indicative of an increase in hydrocarbon chain disorder (Boggs et al., 1984). Therefore, the binding of Ca^{2+} on the sulfate group in SGC resulted in a further weakening of the intermolecular hydrogen bonding and an increase in the intermolecular distance. Again, this difference in chain disorder is most likely due to the non-hydroxy component since the binding of Ca^{2+} to SGC weakened the hydrogen bonding of the amide group of only the non-hydroxy species and not the α-hydroxy species (Figure 4).

In summary, by using high-pressure Fourier transform infrared spectroscopy, we have shown in this study that Ca^{2+} bound to the sulfate group of SGC (Figure 2). The binding of Ca^{2+} to SGC weakened the hydrogen bonding in the polar head region (Figure 4). As a consequence, the SGC hydrocarbon chains increased in mobility (Figures 6 and 7). In contrast, α-hydroxylation of the SGC fatty acid strengthened the hydrogen bonding in the polar head region and as a consequence reduced the effect of Ca^{2+} on the hydrocarbon chain disorder (Figures 4, 6, and 7).

We have shown in this study that the technique of high-pressure Fourier transform infrared spectroscopy could offer a new approach in the study of sulfoglycolipid dynamics. This technique reveals structural information on different regions of the lipid molecule that previously required the use of many techniques. The same experimental approaches could be used in a study on the effects of cation binding to other sulfatides. The study can be performed with lipid multibilayer dispersions as presented in this study; or alternatively, it could be done on isolated membranes or whole cells (Wong et al., 1991). The sulfatide which is of particular interest to us is sulfogalactosylglycerolipid (SGG), which is present selectively in mammalian germ cells (Murray & Narasimhan, 1990). Since Ca^{2+} has been shown to be present on the sperm surface (Roomans, 1975; Ruknudin, 1989) and extracellular Ca^{2+}, as well as Ca^{2+} influx, is significant for inducing the mammalian sperm to gain fertilizing ability (Yanagimachi, 1988), we are interested in determining the role of SGG in these events.

ACKNOWLEDGMENT

We are thankful to Doug Moffat for assistance in data processing and Dr. M. Kates for his expert advice in lipid extraction techniques and his valuable discussion on the manuscript.

REFERENCES

Abramson, M., Katzman, R., Curci, R., Wilson, C. (1967) *Biochemistry 6*, 295–304.

Auger, M., Jarrell, H. C., Smith, I. C. P., Siminovitch, D. J., Mantsch, H. H., & Wong, P. T. T. (1988) *Biochemistry 27*, 6086–6093.

Auger, M., Smith, I. C. P., Mantsch, H. H., & Wong, P. T. T. (1990) *Biochemistry 29*, 2008–2015.
Bellamy, A. A. (1975) *The Infrared Spectra of Complex Molecules*, Vol. 1, 3rd ed., Chapman and Hall, London.
Bentley, J. P., Feeney, L., Hanson, A. N., & Mixon, R. N. (1976) *Invest. Opthalmol. 15*, 575–579.
Boggs, J. M. (1987) *Biochim. Biophys. Acta 906*, 353–404.
Boggs, J. M., Koshy, K. M., & Rangaraj, G. (1984) *Chem. Phys. Lipids 36*, 65–89.
Dreyfus, H., Pieringer, J. A., Farooqui, A. A., Harth, S., Rebel, G., & Sarlieve, L. L. (1978) *J. Neurochem. 30*, 167–174.
Dyer, C. A., & Benjamins, J. A. (1990) *J. Cell Biol. 111*, 625–633.
Farooqui, A. A. (1978) *Int. J. Biochem. 9*, 709–716.
Hakomori, S.-I. (1981) *Annu. Rev. Biochem. 50*, 733–764.
Ishizuka, I., & Yamakawa, T. (1974) *J. Biochem. 76*, 221–223.
Karlsson, K. A., Samuelsson, B. E., & Steen, G. O. (1971) *J. Membr. Biol. 5*, 169–184.
Karlsson, K. A., Leffler, H., & Samuelsson, B. E. (1974) *J. Biol. Chem. 249*, 4819–4823.
Kates, M. (1986) *Techniques in Lipidology*, 2nd ed., pp 102–108 and 172–175, Elsevier, New York.
Koshy, R. M., & Boggs, J. M. (1983) *Chem. Phys. Lipids 34*, 41–53.
Martensson, E. (1963) *Acta Chem. Scand. 17*, 1174–1176.
Morrel, P., Bornstein, M. B., & Norton, W. T. (1972) in *Basic Neurochemistry* (Albers, R. W., Siegel, G. J., Katzman, R., & Aganoff, B. W., Eds.) p 497, Little, Brown, Boston.
Murray, R. K., & Narasimhan, R. (1990) in *Glycolipids, Phosphoglycolipids, and Sulfoglycolipids* (Kates, M., Ed.) pp 321–361, Plenum Press, New York.
Norton, W. T., & Autilo, L. A. (1966) *J. Neurochem. 13*, 213–222.
Nyholm, P. G., Pascher, I., & Sundell, S. (1990) *Chem. Phys. Lipids 52*, 1–10.
Pascher, I. (1976) *Biochim. Biophys. Acta 455*, 443–451.
Pascher, I., & Sundell, S. (1977) *Chem. Phys. Lipids 20*, 175–191.
Pimentel, G. C., & McClellan, A. L. (1960) in *The Hydrogen Bond*, pp 67–141, Freeman, San Francisco.
Quinn, P. J., & Sherman, W. R. (1971) *Biochim. Biophys. Acta 233*, 734–752.
Roomans, G. M. (1975) *Exp. Cell. Res. 96*, 23–30.
Ruknudin, A. (1989) *Gamete Res. 22*, 375–384.
Snyder, R. G. (1961) *J. Mol. Spectrosc. 7*, 116–141.
Stein, R. S., & Sutherland, G. B. B. M. (1953) *J. Chem. Phys. 21*, 370–371.
Stein, R. S., & Sutherland, G. B. B. M. (1954) *J. Chem. Phys. 22*, 1993–1999.
Sung, S. J., Esselman, W. J., & Sweeley, C. C. (1973) *J. Biol. Chem. 248*, 6528–6533.
Wong, P. T. T. (1984) *Annu. Rev. Biophys. Bioeng. 13*, 1–24.
Wong, P. T. T. (1987) in *High Pressure Chemistry and Biochemistry* (van Eldik, R., & Jonas, J., Eds.) pp 381–400, D. Reidel Publishing Co., Boston.
Wong, P. T. T., Moffat, D. J., & Baudais, F. L. (1985) *Appl. Spectrosc. 39*, 733–735.
Wong, P. T. T., Siminovitch, D. J., & Mantsch, H. H. (1988) *Biochim. Biophys. Acta 947*, 139–171.
Wong, P. T. T., Wong, R. K., Caputo, T. A., Godwin, T. A., & Rigas, B. (1991) *Proc. Natl. Acad. Sci. 88*, 10988–10992.
Yanagimachi, R. (1988) in *The Physiology of Reproduction* (Knobil, E., & Neill, J. D., Eds.) pp 135–185, Raven Press, New York.